

Evaluating the Effects of Carbon Nanoreactor Diameter and Internal Structure on the Pathways of the Catalytic Hydrosilylation Reaction

William A. Solomonsz, Graham A. Rance,* and Andrei N. Khlobystov*

Three different types of carbon nanoreactors, double-walled nanotubes (DWNT), multi-walled nanotubes (MWNT) and graphitised carbon nanofibers (GNF) have been appraised for the first time as containers for the reactions of phenylacetylene hydrosilylation catalysed by a confined molecular catalyst $[Rh_4(CO)_{12}]$. Interactions of $[Rh_4(CO)_{12}]$ with carbon nanoreactors determining the ratio of β -addition products are unchanged for all nanoreactors and are virtually unaffected by the confinement of $[Rh_4(CO)_{12}]$ inside carbon nanostructures. Conversely, the relative concentrations of reactants affecting the ratio of addition and dehydrogenative silylation products is very sensitive to nanoscale confinement, with all nanoreactors demonstrating significant effects on the distribution of reaction products as compared to control experiments with the catalyst in bulk solution or adsorbed on the outer surface of nanoreactors. Surprisingly, the widest nanoreactors (GNF) change the reaction pathway most significantly, which is attributed to the graphitic step-edges inside GNF providing effective anchoring points for the catalyst and creating local environments with greatly altered concentrations of reactants as compared to bulk solution. Possessing diameters significantly wider than molecules, GNF impose no restrictions on the transfer of reactants while providing the strongest confinement effects for the reaction. Furthermore, GNF facilitate the effective recyclability of the catalyst and thus represents a superior nanoreactor system to carbon nanotubes.

1. Introduction

Carbon nanoreactors represent the ultimate class of hollow nanostructured materials to utilise nanoscale spatial

confinement to control the pathways of chemical reactions.^[1–4] Possessing superior mechanical, chemical and thermal stabilities relative to zeolites, nanoporous solids and molecular containers, carbon nanoreactors are able to encapsulate the most expansive array of guest molecules driven into the internal cavity via ubiquitous van der Waals forces^[5,6] and as such have been successfully employed as nanoscale reaction vessels to examine the effects of confinement on both single-molecule and preparative chemical transformations.^[7–17] For example, it has been shown that carbon nanoreactors facilitate the formation of unique molecular products, such as linear oligomers of fullerene epoxide^[8] and dynamic dimers of [60]fullerene^[9] inside single-walled carbon nanotubes (SWNT), which are precluded by bulk synthetic approaches. Further studies conducted using MWNT, which possess a wider internal channel and thus the opportunity to selectively incarcerate transition metal nanoparticle (NP) catalysts,^[18] have additionally shown

W. A. Solomonsz, Dr. G. A. Rance,
Prof. A. N. Khlobystov
School of Chemistry
University of Nottingham
University Park
Nottingham, NG7 2RD, U.K
E-mail: Graham.Rance@nottingham.ac.uk;
Andrei.Khlobystov@nottingham.ac.uk

Prof. A. N. Khlobystov
Nottingham Nanoscience & Nanotechnology Centre
University of Nottingham
University Park
Nottingham, NG7 2RD, U.K

DOI: 10.1002/sml.201302732



that the enhancement in activity and selectivity of the confined catalysts in the PtNP-catalysed asymmetric hydrogenation of α -ketoesters,^[12] the RhPtNP-catalysed hydrogenation of cinnamaldehyde^[14] and the RhNP-catalysed conversion of syngas to ethanol^[15] is related to confinement in carbon nanoreactors. These effects relate to the pairwise interactions between the host nanoreactor and the components of the confined reaction (reactants and catalyst) and result in drastically altered concentrations, pressures and alignment of reactant molecules as compared to the bulk solution or gas phase and are understood to become increasingly important as the dimensions of the host container approach commensuration with the size of the guest molecules.^[1–4]

Surprisingly, larger nanocontainers with diameters exceeding the size of reactant molecules by a factor of 50 or more have also recently been found to fundamentally alter the mechanisms of preparative chemical reactions. Hollow graphitised carbon nanofibers (GNF) are significantly wider than MWNT (internal diameters typically above 50 nm) and thus facilitate effective transport of molecules through the tubular structure.^[19–23] Furthermore, their distinctive internal surface, consisting of a succession of 3–4 nm high steps formed by rolled-up sheets of graphene, provides effective adsorption loci for catalytic nanoparticles^[24] and therefore localised nanoscale reaction environments, different to the bulk phase, which mimic those observed in much narrower carbon nanostructures. Our studies have shown that the selectivity,^[19,20] activity^[21] and recyclability^[21] of the catalysts in preparative synthesis can be tuned in GNF while Fickian diffusion of reactants/products to/from such nanoreactors remains unrestricted. Recently, we reported the first observation of regioselectivity switching due to spatial confinement of catalytic centres in GNF using the hydrosilylation of terminal alkynes as a model reaction. Systematic comparison of the catalytic properties of Rh and RhPt nanoparticles embedded in carbon nanoreactors with free-standing and surface-adsorbed nanoparticles showed that the directions of reactions inside GNF are largely controlled by the specific non-covalent π - π interactions between aromatic reactant molecules and the nanofiber channel increasing the local concentration of the reactant in GNF.^[20]

Changing the pathways of chemical transformations inside carbon nanoreactors, a key emerging branch of chemical nanosciences, has often been accounted for by the structural characteristics of the nanoreactor and thus the specific interactions between nanoreactor-catalysts and nanoreactor-reactants.^[1–4] While many important examples of chemical reactions inside nanotubes have been reported, all of them remain sporadic as no attempts to compare different types of nanoreactors for the same transformation and the same type of catalyst have been made to date. Since systematic comparison of nanoreactors with different diameters and morphology is essential for understanding the fundamental aspects of nanoscale confinement and developing real practical applications of carbon nanoreactors, in this novel study we investigate the hydrosilylation reaction of phenylacetylene and triethylsilane in the presence of a $[\text{Rh}_4(\text{CO})_{12}]$ catalyst in three different types of nanoreactors. The molecular catalyst $[\text{Rh}_4(\text{CO})_{12}]$ was inserted for the first time into

DWNT, MWNT and GNF and the regioselectivity of the hydrosilylation reaction was studied at different degrees of confinement and compared to the reactions of unconfined catalysts. Our innovative study demonstrates that the pathways of preparative chemical reactions can be effectively controlled by the diameter and internal structure of the carbon nanoreactor.

2. Results and Discussion

2.1. Preparation of Nanoreactors

The hydrosilylation of phenylacetylene by hydrosilanes is generally catalysed by Pt group metals, in particular rhodium,^[20,25] platinum^[26] ruthenium,^[27] and iridium^[28] and yields commercially valuable products^[29] in a specific distribution depending on the nature of the catalyst and the experimental conditions.^[30] Our study requires a catalyst that possesses both high versatility and activity at low loadings^[31] and exemplary stability to the conditions required for encapsulation in a wide range of host carbon nanoreactors (see S1 and S2 in the Supporting Information);^[32] hence, we selected the molecular catalyst tetrarhodium dodecacarbonyl as it both fulfilled these requirements and exhibited the most suitable catalytic properties in the hydrosilylation reaction (see S3 and S4 in the Supporting Information). The chosen $[\text{Rh}_4(\text{CO})_{12}]$ catalyst was vaporised at reduced pressure in the presence of open and dry carbon nanocontainers (DWNT, MWNT and GNF) in order to facilitate the transport and subsequent encapsulation of gaseous $[\text{Rh}_4(\text{CO})_{12}]$ molecules inside the internal cavities of the hollow carbon structures. Once the composite material was cooled to ambient temperature and pressure, the molecules solidified inside nanoreactors to form $[\text{Rh}_4(\text{CO})_{12}]@\text{DWNT}$, $[\text{Rh}_4(\text{CO})_{12}]@\text{MWNT}$ and $[\text{Rh}_4(\text{CO})_{12}]@\text{GNF}$ nanoreactors respectively. The loading of molecular catalyst was optimised within each of these containers (see Table S1 in the Supporting Information), such that the metal content was maximised with the majority (>90%) of the catalyst molecules residing inside the nanoreactors. Increasing the loading beyond these optimal values resulted in the inherent inability to control the location of the catalytic centres.

High resolution transmission electron microscopy (HR-TEM, **Figure 1** and Figure S1 in the Supporting Information) was used as the primary characterisation technique for these structures,^[32–35] clearly showing that the catalyst is evenly distributed along the length of the internal channel of DWNT and MWNT in spite of their narrow diameter. The molecular catalysts are stabilised by van der Waals interactions with the concave side of the CNT (which are greater as compared to the convex side),^[1] whereas in GNF the catalyst molecules are immobilised at the internal graphitic step-edges (Figures 1f–g and 3). In a control experiment, $[\text{Rh}_4(\text{CO})_{12}]$ was deposited selectively onto the exterior of DWNT filled with fullerene C_{60} , blocking all of the internal space in nanotubes, prior to the addition of $[\text{Rh}_4(\text{CO})_{12}]$ ($[\text{Rh}_4(\text{CO})_{12}]/\text{DWNT}$, Figure S1 in the Supporting Information). Systematic comparison of $[\text{Rh}_4(\text{CO})_{12}]@\text{DWNT}$ and $[\text{Rh}_4(\text{CO})_{12}]/$

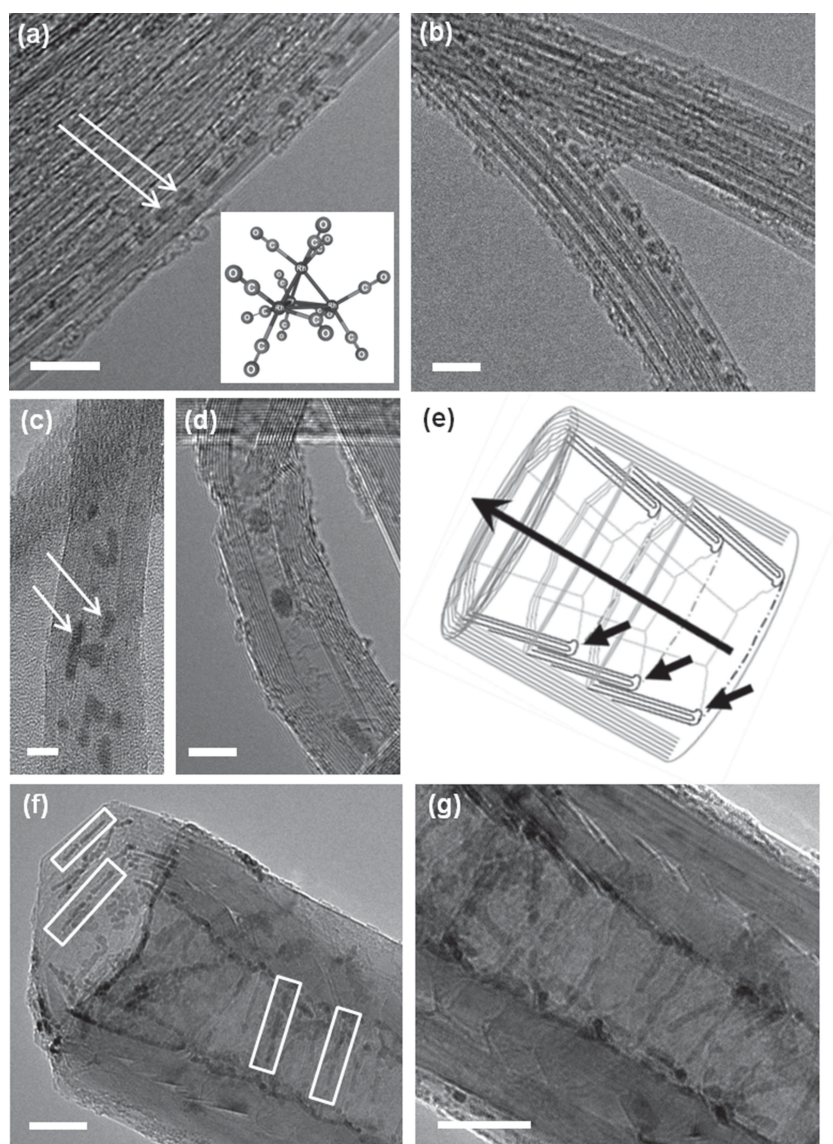


Figure 1. HR-TEM images of (a)–(b) $[\text{Rh}_4(\text{CO})_{12}]@\text{DWNT}$, (c)–(d) $[\text{Rh}_4(\text{CO})_{12}]@\text{MWNT}$ and (f)–(g) $[\text{Rh}_4(\text{CO})_{12}]@\text{GNF}$ nanoreactors. The internal diameters of DWNT, MWNT and GNF are 1.3 ± 0.5 nm, 5.3 ± 3.3 nm and 52.7 ± 16.2 nm respectively. The embedded catalyst molecules (inset in panel a) appear as dark clusters after decomposition and coalescence induced by electron beam radiation: (a–d) anchored to the nanotube sidewall (highlighted by white arrows) and (f,g) residing along the graphitic step-edges (highlighted by white boxes). A schematic representation of the GNF structure (e) highlights the unique internal structure of this hybrid nanomaterial, comprising graphitic step-edges suitable for catalyst deposition (highlighted by black arrows). Scale bars are 5 nm (a–d) and 20 nm (f–g).

DWNT enables discrimination between the effects of catalyst support and confinement in nanoreactors. Most importantly, appraisal of $[\text{Rh}_4(\text{CO})_{12}]@\text{DWNT}$, $[\text{Rh}_4(\text{CO})_{12}]@\text{MWNT}$ and $[\text{Rh}_4(\text{CO})_{12}]@\text{GNF}$ will enable, for the first time,

mediate **A** in preference to intermediate **B** (**Scheme 2**). This leads to the preferential formation of the more thermodynamically stable β -(*E*) isomer so as to remove the destabilising steric repulsion between adjacent Ph and SiEt_3

a comparison between the confinement effects in carbon nanoreactors of different sizes and morphologies (**Table 1**).

2.2. Hydrosilylation Reaction

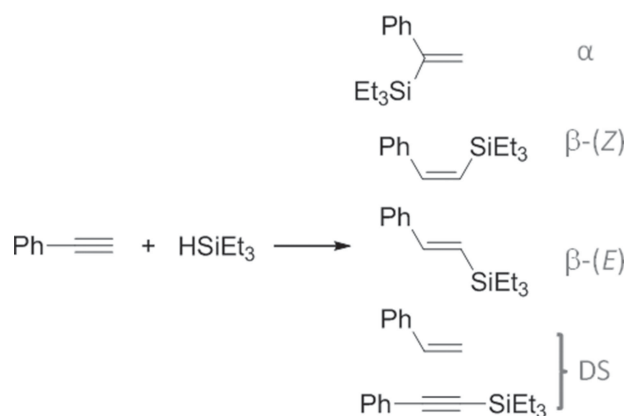
The hydrosilylation of triethylsilane across phenylacetylene is highly suitable for testing the properties of different nanoreactors as the reaction does not proceed in the absence of rhodium and therefore controlled positioning of the molecular catalytic centres (i.e., inside for $[\text{Rh}_4(\text{CO})_{12}]@\text{DWNT}$ and outside for $[\text{Rh}_4(\text{CO})_{12}]/\text{DWNT}$) ensures that the reaction locus is well defined. Furthermore, rhodium chemistry dictates that the hydrosilylation reaction proceeds via different pathways to yield all five possible products (**Scheme 1**)^[20,27,36] each of which may be quantified by ^1H NMR spectroscopy (see S5 in the Supporting Information) and thus provides a comprehensive chemical probe for the effects of nanoreactors on the pathways of catalytic reactions.

The relative ratio of β addition products provides an important insight into the reaction pathway. Comparison of the β -(*Z*): β -(*E*) ratios of the “free” molecular $[\text{Rh}_4(\text{CO})_{12}]$ catalyst compared to the supported ($[\text{Rh}_4(\text{CO})_{12}]/\text{DWNT}$) and confined ($[\text{Rh}_4(\text{CO})_{12}]@\text{DWNT}$) catalysts shows that the environment of the catalyst alters this ratio. When the catalyst is supported on the surface or confined inside the DWNT, there is a 2-fold promotion of the *trans* product of β addition (β -(*E*) product) compared to the bulk (**Table 2**, entries 1–3 and **Figure 2a**).

This shows that the interactions between carbon nanotubes and the catalyst molecules, irrespective of their location (in or on nanoreactors), sufficiently changes the nature of the catalyst and results in the stabilisation of the inter-

Table 1. The unique properties of DWNT, MWNT and GNF as carbon nanoreactors operating under the Fickian diffusion regime.

| | DWNT | MWNT | GNF |
|---------------------------|--|--|---|
| Catalyst environment | Stabilised by van der Waals interactions with the concave interior | Stabilised by van der Waals interactions with the concave interior | Immobilised internally at the graphitic step-edges |
| Accessibility of interior | Transport resistance due to extreme spatial confinement | Low diffusion barrier due to the wide inner channel | Low diffusion barrier due to the extremely wide inner channel |



Scheme 1. Reaction scheme for the hydrosilylation of phenylacetylene and triethylsilane yielding a distribution of three addition products (α , β - Z and β - E) and two dehydrogenative silylation products (DS), which are produced in equimolar quantities.

Table 2. The effect of catalyst environment on the comparative selectivity for the products of hydrosilylation of phenylacetylene and triethylsilane. Comparative TOF values for these catalytic systems are presented in S4 of the Supporting Information file. All reactions were performed at a normalised catalyst loading of 2.7 mmol% $[\text{Rh}_4(\text{CO})_{12}]$.

| Catalyst | Container | Regioselectivity | |
|---------------------------------|-----------|-------------------------------|-------------------|
| | | β - Z : β - E | β - Z :DS |
| $[\text{Rh}_4(\text{CO})_{12}]$ | “free” | 1.1:1 | 9.3:1 |
| $[\text{Rh}_4(\text{CO})_{12}]$ | /DWNT | 0.6:1 | 3.5:1 |
| $[\text{Rh}_4(\text{CO})_{12}]$ | @DWNT | 0.5:1 | 2.2:1 |
| $[\text{Rh}_4(\text{CO})_{12}]$ | @MWNT | 0.5:1 | 2.0:1 |
| $[\text{Rh}_4(\text{CO})_{12}]$ | @GNF | 0.5:1 | 1.1:1 |

groups in intermediate **B**. This effect appears to be somewhat universal and independent of the internal diameter and internal structure of the carbon container the $[\text{Rh}_4(\text{CO})_{12}]$ is anchored to, with a similar change in β - Z : β - E also observed for reactions confined in MWNT and GNF (Table 2, entries 4–5). Although the intermediate stability appears to be unaffected by confinement, consistent with our previous studies regarding the nanoparticle-catalysed hydrosilylation of phenylacetylene by triethylsilane in carbon nanoreactors,^[20] manipulation of the ratio of β addition products as

a consequence of catalyst-nanotube interactions is a general phenomenon applicable to variety of carbon nanoreactors and consequently can be harnessed for the efficient promotion of the β - E product (Figure 2).

However, although the relative stabilities of intermediates **A** and **B** are unaffected by confinement of the $[\text{Rh}_4(\text{CO})_{12}]$ catalyst as compared to the supported species, the overall product distribution is fundamentally altered upon confinement. The β - Z :DS ratio is a useful diagnostic parameter to assess the fate of intermediate **B** and hence probe the effects of confinement as this ratio is related to the concentrations of triethylsilane and phenylacetylene. Dehydrogenative silylation (DS) products are formed in this reaction due to the β -H elimination process (Scheme 2), the viability of which can be influenced by changes in the relative concentrations of reactant molecules,^[20] present in equimolar quantities in the feedstock solution (bulk phase). Our measurements show that confinement of the reaction inside $[\text{Rh}_4(\text{CO})_{12}]$ @DWNT nanoreactors leads to a decrease in the β - Z :DS ratio, i.e., a promotion of DS products, compared to the reaction on the surface of $[\text{Rh}_4(\text{CO})_{12}]$ /DWNT and “free” $[\text{Rh}_4(\text{CO})_{12}]$ (Table 2). This indicates that the concentration of aromatic reactants is increased inside DWNT, changing the pathway of this reaction. This observation is consistent with our previous studies using RhNP@GNF nanoreactors, where a 3-fold increase of local concentration of phenylacetylene inside nanoreactors resulted in the promotion of the β -H elimination step so as to consume the excess of aromatic alkyne.^[20] It is important to note that this effect is observed as phenylacetylene is the only reactant that possesses aromaticity and is thus favourably encapsulated at the expense of the aliphatic silane inside the DWNT nanoreactors, which are known to have a special affinity for aromatic species.^[22,23,37–39]

Such an effect had only previously been observed inside GNF nanoreactors, which are also much more accessible than DWNT for preparative reactions due to their wider and thus less restrictive inner channel. Therefore, building on the discovery that all sizes and shapes of nanocontainer can be used as preparative vessels upon encapsulation of a suitable catalyst, the hydrosilylation reaction studied here yielded a unique opportunity to assess selectivity switching in different types of hollow carbon nanocontainers and thus to examine the extent of confinement as a function of nanoreactor

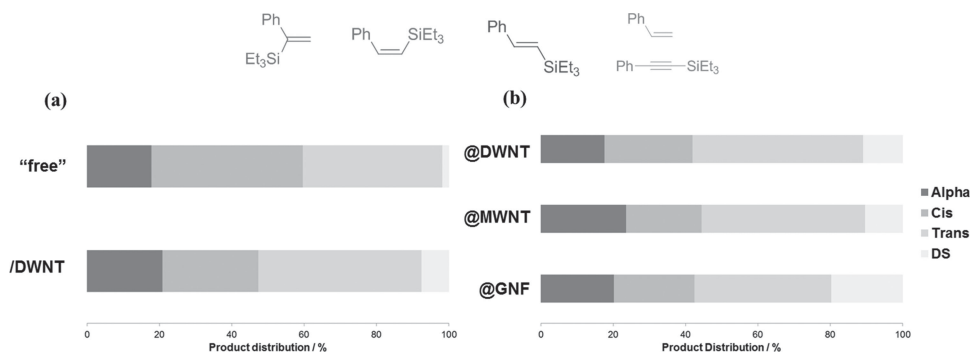
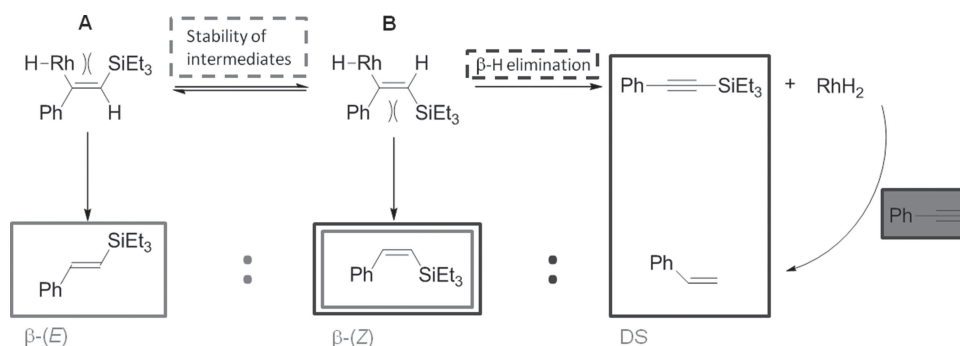


Figure 2. Graphical distributions of shifts in regioselectivity upon supporting the catalyst, where a promotion of the β - E product is observed (a) and confining the catalyst within carbon nanoreactors of varying diameter and morphologies, where GNF are found to show the largest shift in regioselectivity compared to the bulk, observed via promotion of the DS products (b).



Scheme 2. The β -(Z): β -(E) ratio is an indication of the relative stability of intermediates **A** and **B** (light boxes) whilst the β -(Z):DS ratio is related to the favourability of the β -H elimination step (dark boxes), so as to deplete the excess of phenylacetylene.

diameter (comparison of DWNT and MWNT) and internal structure (comparison of CNT and GNF). This was achieved by evaluating the β -(Z):DS ratio for $[\text{Rh}_4(\text{CO})_{12}]$ in DWNT, MWNT and GNF nanoreactors (Table 1), where it was startling to discover that not only are the pathways of the hydrosilylation reaction altered (as compared to the bulk) inside all of the nanoreactors, but that the most extreme effect was observed inside $[\text{Rh}_4(\text{CO})_{12}]$ @GNF nanoreactors (Table 2 and Figure 2b) despite the fact that they are the widest nanoreactors in this study. Our measurements have shown that there is a 2-fold decrease in the β -(Z):DS ratio inside GNF compared to both DWNT and MWNT, in addition to the 4-fold decrease these nanoreactors show compared to the bulk.

As the internal diameter of DWNT is close to the size of small organic molecules (the critical van der Waals diameters of phenylacetylene, triethylsilane and tetrarhodium dodecacarbonyl are 0.42, 0.53 and 0.93 nm respectively), the energy of encapsulation of reactants (E_c) is significantly greater than the energy of their adsorption on DWNT surface (E_a),^[2] and thus the greatest enhancement in reactant concentration was expected to be in DWNT leading to a greater proportion of DS products as compared to MWNT and other wider nanoreactors. However, our results show that there is effectively no difference in the β -(Z):DS ratio for reactions in DWNT and MWNT. This indicates that local concentration effects are independent of carbon nanotube diameter, where the effect of higher E_c in narrow diameter nanostructures such as DWNT (relative to MWNT) is offset by a corresponding reduction in the rate of mass transfer of reactants (k_c) which will be higher in wider MWNT (relative to DWNT). Consequently, as the greater than 8-fold selectivity switch in GNF as compared to the bulk cannot be explained by nanoreactor diameter, this effect must be related to the unique step-edged

internal structure of the GNF nanoreactors, where the combination of high mass transfer and high energy of step-edge encapsulation (E_c') creates local reaction environments that concentrates an even greater excess of phenylacetylene than can be seen in CNT which possess an atomically smooth interior (**Figure 3**).

The increased concentration of phenylacetylene and the subsequent preferential β -H elimination step in nanoreactors is related to the specific π - π interactions^[40] between the phenyl ring and the graphitic surface of the interior of the carbon nanocontainer, which is not available for fully aliphatic triethylsilane molecules. Our results suggest that the

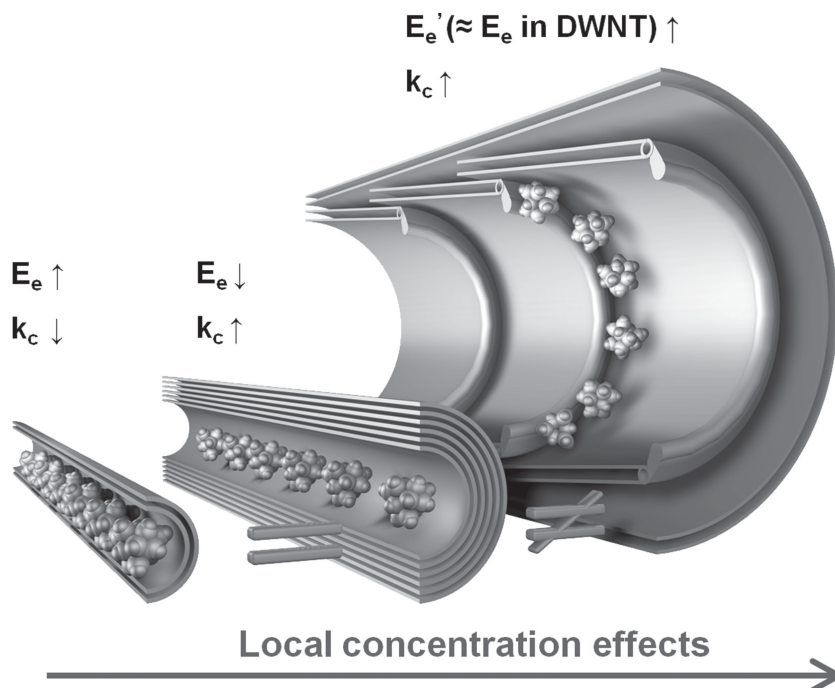


Figure 3. Schematic representation of the contrasting internal environments of $[\text{Rh}_4(\text{CO})_{12}]$ @DWNT, $[\text{Rh}_4(\text{CO})_{12}]$ @MWNT and $[\text{Rh}_4(\text{CO})_{12}]$ @GNF (from left to right, respectively) and the relative local concentration effects induced inside these nanoreactors. The observed effects are the result of a balance between the energy of encapsulation in CNT (E_c) and step-edge encapsulation in GNF (E_c') with the mass transfer rate (k_c) of reactants (compared relative to DWNT). The most extreme effects are observed inside the internally corrugated GNF, whereas the net effects in CNT are minimised, because the step-edge encapsulation provides a similarly constrained environment as in DWNT, but the wide diameters of GNF have the additional ability to readily facilitate the rapid Fickian diffusion of reagents.

most preferential interactions occur within GNF (Figure 3), causing significant mechanistic deviations (Scheme 2), whilst these nanoreactors also boast a more accessible internal cavity than CNT. Furthermore, as a consequence of the stability of the nanoreactor-catalyst interface inside GNF, the catalyst in GNF can be recyclable (see S6 in the Supporting Information). TEM analysis of the $[\text{Rh}_4(\text{CO})_{12}]$ @GNF catalyst after one reaction cycle provides a snapshot of the reaction, frozen in time, where the catalytic material persists within the inner channel after catalysis due to anchoring at the graphitic step-edges and the reaction products are observed as amorphous material within the GNF nanoreactor interior containing C and Si, as confirmed by energy dispersive X-ray spectroscopy. Therefore, GNF represent the ultimate container for preparative chemical transformations.

3. Conclusion

Carrying out reactions inside carbon nanoreactors offers an elegant tool to alter the pathways of conventional organic transformations to yield products different to the bulk. In this study, we probed nanoreactor-catalyst and nanoreactor-reactant interactions via synthesis of novel $[\text{Rh}_4(\text{CO})_{12}]$ -based catalytic systems allowing hydrosilylation reactions to be performed either inside or outside the DWNT. We demonstrate that preparative, molecular-catalysed hydrosilylation reactions on the exterior and interior of DWNT follow a different reaction pathway to the bulk, as observed by a change in the β -(Z): β -(E) products ratio. This ratio is unaffected by confining the reaction inside DWNT showing similar value to other, wider nanoreactors MWNT and GNF, implying that nanoreactor-catalyst interactions determine the ratio of these products regardless of the location of catalyst (inside or outside nanoreactor) or size of nanoreactor. In contrast, ratio of β -(Z):DS products, controlled by local concentration effects, shows that the most extreme switch in product selectivity occurs inside GNF. We demonstrate that confinement effects invoked by divergent local concentrations are universally observed inside all carbon nanocontainers, although GNF appear to have the potential to be superior nanoreactors as compared to DWNT and MWNT. Controlling the pathways of catalytic chemical transformations is the pinnacle goal of the chemist and typically involves time and skill intensive functionalisation of molecules; our results show that non-covalent interactions of reagents with carbon nanoreactors – essential for controlled assembly at the nanoscale^[41,42] – provides a superior alternative approach and may ultimately facilitate the formation of novel molecular structures inaccessible by other means.

4. Experimental Section

General: All reagents were purchased from Sigma-Aldrich, UK and used without further purification. Double-walled carbon nanotubes (CVD, Times Nano, Chengdu Organic Chemicals, China), multi-walled carbon nanotubes (CVD, PD30L520, NanoLab, USA)

and graphitised carbon nanofibers (CVD, Pyrograf PR-19, Applied Science, USA) were obtained from commercial sources. All glassware was cleaned with a mixture of hydrochloric and nitric acid (3:1 v/v, 'aqua regia') and rinsed thoroughly with deionised water, cleaned with potassium hydroxide in isopropyl alcohol and finally rinsed thoroughly with deionised water. ^1H NMR spectra were obtained using a Bruker DPX-300 (300.13 MHz) spectrometer at 298K using CDCl_3 as the solvent. Thermogravimetric analysis (TGA) was performed using a TA Instruments SDT Q600 under a flow of air at a rate of 100 mL min^{-1} at a heating rate of $10 \text{ }^\circ\text{C min}^{-1}$ from room temperature to $900 \text{ }^\circ\text{C}$. Transmission electron microscopy (TEM) was performed using a JEOL 2100F TEM (field emission gun source, information limit $<0.19 \text{ nm}$) operated at 100 kV accelerating voltage at room temperature. Energy dispersive X-ray (EDX) analysis was performed using an Oxford Instruments INCA 560 X-ray microanalysis system. Samples were prepared via drop-drying methanolic solutions onto a copper grid mounted "lacey" carbon films.

Synthesis of Nanoreactor Catalysts: To the DWNT_{45%} (10.0 mg, see S1.1.1 in the Supporting Information), MWNT_{40%} (6.7 mg, see S1.2.1 in the Supporting Information) or GNF (7.13 mg, annealed for 1 hr at $450 \text{ }^\circ\text{C}$ in air) was immediately added tetrarhodium dodecacarbonyl (1.0 mg, 0.30 mg or 0.50 mg respectively), sealed under vacuum (10^{-6} mbar) in a Pyrex ampoule and heated at $140 \text{ }^\circ\text{C}$ for 72 hours to ensure complete vaporisation and penetration of the tetrarhodium dodecacarbonyl into the hollow interior of the carbon nanostructures. The samples were cooled and then stirred in tetrahydrofuran (15 mL) at room temperature for 1 hour in order to remove any metal carbonyl from the exterior of the carbon nanostructures. The products were collected by vacuum filtration (0.45 μm , PTFE), washed with tetrahydrofuran (75 mL) and dried *in vacuo* to yield dark solids (10.6 mg, 5.5 mg and 7.5 mg respectively).

The Hydrosilylation Reaction: In a typical experiment, to an argon-flushed Schlenk tube was added the catalyst (2.7 mmol% $[\text{Rh}_4(\text{CO})_{12}]$), triethylsilane (0.72 mL, 4.5 mmol, 1 eq.) and to this was added dropwise phenylacetylene (0.50 mL, 4.5 mmol, 1 eq.). The mixture was homogenised by bath sonication at room temperature and then stirred at $90 \text{ }^\circ\text{C}$. The progress of the reaction was monitored by ^1H NMR spectroscopy and product distributions were generated by integrating the one-proton doublets of each product, which have unique shifts which were found to match known literature values.^[29]

Supporting Information

Supporting Information is available from the Wiley Online Library or from the author.

Acknowledgements

This work was supported by the European Research Council (ERC), Engineering and Physical Science Research Council (EPSRC), Royal Society and Nottingham Nanoscience & Nanotechnology Centre

(NNNC). The authors would also like to thank Mr Scott Miners for assistance with manuscript preparation.

- [1] X. Pan, X. Bao, *Acc. Chem. Res.* **2011**, *44*, 553.
- [2] D. A. Britz, A. N. Khlobystov, *Chem. Soc. Rev.* **2006**, *35*, 637.
- [3] P. Serp, E. Castillejos, *ChemCatChem* **2010**, *2*, 41.
- [4] A. N. Khlobystov, *ACS Nano* **2011**, *5*, 9306.
- [5] G. Borsato, J. Rebek Jr., A. Scarso, in *Selective Nanocatalysts and Nanoscience*, (Eds: A. Zecchina, S. Bordiga, E. Groppo), WILEY-VCH, Weinheim, Germany **2011**, pp. 105–108.
- [6] *Molecular Encapsulation: Organic Reactions in Constrained Systems*, (Eds: U. H. Brinker, J.-L. Miesusset), Wiley, New York **2010**.
- [7] D. A. Britz, A. N. Khlobystov, J. Wang, A. S. O'Neil, M. Poliakoff, A. Ardavan, G. A. D. Briggs, *Chem. Commun.* **2004**, 176.
- [8] D. A. Britz, A. N. Khlobystov, K. Porfyrakis, A. Ardavan, G. A. D. Briggs, *Chem. Commun.* **2005**, 37.
- [9] E. Nakamura, M. Koshino, T. Saito, Y. Niimi, K. Suenaga, Y. Matsuo, *J. Am. Chem. Soc.* **2011**, *133*, 14151.
- [10] M. Koshino, Y. Niimi, E. Nakamura, H. Kataura, T. Okazaki, K. Suenaga, S. Iijima, *Nature Chem.* **2010**, *2*, 117.
- [11] S. Miners, G. A. Rance, A. N. Khlobystov, *Chem. Commun.* **2013**, *49*, 5586.
- [12] H. Zhang, X. Pan, X. Han, X. Liu, X. Wang, W. Shen, X. Bao, *Chem. Sci.* **2013**, *4*, 1075.
- [13] Z. Chen, Z. Guan, M. Li, Q. Yang, C. Li, *Angew. Chem. Int. Ed.* **2011**, *50*, 4913.
- [14] J. Teddy, A. Falqui, A. Corrias, D. Carta, P. Lecante, I. Gerber, P. Serp, *J. Catal.* **2011**, *278*, 59.
- [15] X. Pan, Z. Fan, W. Chen, Y. Ding, H. Luo, X. Bao, *Nature Mater.* **2007**, *6*, 507.
- [16] S. Guo, X. Pan, H. Gao, Z. Yang, J. Zhao, X. Bao, *Chem. Eur. J.* **2010**, *16*, 5379.
- [17] H. Yang, S. Song, R. Rao, X. Wang, Q. Yu, A. Zhang, *J. Mol. Catal.:* **2010**, *323*, 33.
- [18] A. La Torre, G. A. Rance, J. El Harfi, J. Li, D. J. Irvine, P. D. Drown, A. N. Khlobystov, *Nanoscale* **2010**, *2*, 1006.
- [19] A. La Torre, M. C. Gimenez-Lopez, M. Fay, G. A. Rance, W. A. Solomonsz, T. W. Chamberlain, P. D. Brown, A. N. Khlobystov, *ACS Nano* **2012**, *6*, 2000.
- [20] W. A. Solomonsz, G. A. Rance, M. Suyetin, A. La Torre, E. Bichoutskaia, A. N. Khlobystov, *Chem. Eur. J.* **2012**, *18*, 13180.
- [21] G. A. Rance, W. A. Solomonsz, A. N. Khlobystov, *Chem. Commun.* **2013**, 1067.
- [22] E. Castillejos, P.-J. Deboutiere, L. Roiban, A. Solhy, V. Martinez, Y. Kihn, O. Ersen, K. Philippot, B. Chaudret, P. Serp, *Angew. Chem. Int. Ed.* **2009**, *48*, 2529.
- [23] E. Castillejos, R. Chico, R. Bacsá, S. Coco, P. Espinet, M. Perez-Cadenas, A. Guerrero-Ruiz, I. Rodriguez-Ramos, P. Serp, *Eur. J. Inorg. Chem.* **2010**, 5096.
- [24] A. La Torre, M. Fay, G. A. Rance, M. C. Gimenez-Lopez, W. A. Solomonsz, P. D. Brown, A. N. Khlobystov, *Small* **2012**, *8*, 1222.
- [25] Y. Goldberg, H. Alper, *Tet. Lett.* **1995**, *36*, 369.
- [26] L. Lewis, K. Sy, G. Bryant, P. Donahue, *Organometallics* **1991**, *10*, 3750.
- [27] M. Jiménez, J. Pérez-Torrente, M. Bartolomé, V. Gierz, F. Lahoz, L. Oro, *Organometallics* **2008**, *27*, 224.
- [28] R. S. Tanke, R. H. Crabtree, *J. Am. Chem. Soc.* **1990**, *112*, 7894.
- [29] I. Fleming, J. Dunogues, R. Smithers, *Org. React.* **1989**, *37*, 57.
- [30] R. Takeuchi, N. Tanouchi, *J. Chem. Soc. Perkin Trans. 1* **1994**, 2909.
- [31] I. Ojima, R. J. Donovan, N. Clos, *Organometallics* **1991**, *10*, 2606.
- [32] T. W. Chamberlain, T. Zoberbier, J. Biskupek, A. Botos, U. Kaiser, A. N. Khlobystov, *Chem. Sci.* **2012**, *3*, 1919.
- [33] D. V. Kazachkin, Y. Nishimura, H. A. Witek, S. Irle, E. Borguet, *J. Am. Chem. Soc.* **2011**, *133*, 8191.
- [34] T. Zoberbier, T. W. Chamberlain, J. Biskupek, N. Kuganathan, S. Eyhusen, E. Bichoutskaia, U. Kaiser, A. N. Khlobystov, *J. Am. Chem. Soc.* **2012**, *134*, 3073.
- [35] Z. Xu, H. Li, K. Fujisawa, Y. A. Kim, M. Endo, F. Ding, *Nanoscale* **2012**, *4*, 130.
- [36] C.-H. Jun, R. Crabtree, *J. Organomet. Chem.* **1993**, *447*, 177.
- [37] R. J. Chen, Y. G. Zhang, D. W. Wang, H. J. Dai, *J. Am. Chem. Soc.* **2001**, *123*, 3838.
- [38] Y. Gao, G. Hu, W. Zhang, D. Ma, X. Bao, *Dalton Trans.* **2011**, *40*, 4542.
- [39] C. Vriamont, M. Devillers, O. Riant, S. Hermans, *Chem. Eur. J.* **2013**, *19*, 12009.
- [40] C. R. Martinez, B. L. Iverson, *Chem. Sci.* **2012**, *3*, 2191.
- [41] L. Tang, X. Yang, *J. Phys. Chem. C* **2012**, *116*, 11783.
- [42] Z. Xu, X. Yang, Z. Yang, *Nano Lett.* **2010**, *10*, 985.

Received: August 20, 2013
Revised: November 29, 2013
Published online: January 25, 2014